COMPARISON BETWEEN X-RAY TUBE BASED AND SYNCHROTRON RADIATION BASED **µCT**

Oliver BRUNKE,
GE Sensing & Inspection Technologies GmbH, phoenix|x-ray, Wunstorf, Germany

Abstract

Nowadays, X-ray tube-based high-resolution CT systems are widely used in scientific research and industrial applications. But the potential, convenience and economy of these lab systems is often underestimated. The present paper shows the comparison of sophisticated conventional µCT with synchrotron radiation-based µCT (SRµCT). The different aspects and characteristics of both approaches like spatial and density resolution, penetration depth, scanning time or sample size is described in detail. The tube-based µCT measurements were performed with a granite-based phoenix nanotom CT system (GE Sensing & Inspection Technologies, Wunstorf, Germany) equipped with a 180 kV – 15 W high-power nanofocus tube with tungsten or molybdenum targets. The tube offers a wide range of applications from scanning low absorbing samples in nanofocus mode with voxel sizes below 500 nm and strong absorbing objects in the high power mode with focal spot and voxel sizes of a few microns. The SRµCT measurements were carried out with the absorption contrast set-up at the beamlines W 2 and BW 2 at HASYLAB/DESY (Hamburg, Germany), operated by the GKSS Research Center. The range of samples examined covers materials of very different absorption levels and related photon energies for the CT scans. Both quantitative and qualitative comparisons of CT scans using composites from the field of materials science are shown.

Keywords: X-ray tube CT system, synchrotron radiation-based CT, comparison, nanofocus X-ray tube, bone architecture, composite microstructure

1. Introduction

High resolution CT nowadays is a well established method for numerous industrial applications [1][2][3] as well as wide range of research areas [4][5]. For both fields the choice of the optimal method is strongly driven by many different factors like sample size and composition, required spatial and contrast resolution or scanning volume and time, etc.

For example in today's quality market, achieving the smallest feature recognition possible in the inspection process has become a higher priority than ever before. Due to complex geometries and miniaturization of many high reliability components in the automotive, electronics and aerospace industries, achieving this level of feature recognition has also become increasingly difficult. CT techniques are used to measure internal distances or the internal wall thickness of complex castings and areas which are often inaccessible for optical scanners or conventional tactile coordinate measurement machines. The CT volume data provides information for reverse engineering or first article inspection of the entire part by merging it with the CAD model to generate a variance map of both data sets [6][7][8]. Combined, these capabilities contribute to early detection of process and product weaknesses therefore increasing yield and productivity.

Regarding high resolution computed tomography with voxel sizes of a few microns or even in the submicron range the state of the art benchmark is defined by CT setups which use synchrotron radiation for the X-ray source. Synchrotron radiation based CT was introduced in the 1980s by Bonse et al [9]. Nowadays it is a standard experiment for users from scientific research as well as industry at numerous Synchrotron laboratories worldwide. The main advantages of these setups are the highly collimated and almost parallel beam and the photon flux which is several orders of

magnitude higher than for conventional X-ray sources. Due to this high flux monochromators can be effectively used to perform CT scans with monochromatic radiation at the desired energy level.

However, in recent years major steps in important hardware components like open microfocus or even nanofocus X-ray tube technology (the later was commercially introduced the first time by phoenix|x-ray in 2001) on the one side and the development of highly efficient and large flat panel detectors (by e.g. GE, Perkin-Elmer, Varian or Hamamatsu) using CCD or CMOS technology on the other, allowed the development of very versatile and high resolution laboratory CT systems like the nanotom (see next section) which are commercially available. Electromagnetic focusing of the electron beam allows generating X-ray beams with an emission spot diameter down to well below one µm which is essential for CT examination with voxels in the sub-micron range. These characteristics principally allow CT measurements which, with respect to spatial resolution, can compete with many absorption contrast setups at synchrotron radiation facilities [10]. The advantages of laboratory X-ray tube based setups like e.g. its accessibility, user-friendliness, high cost effectiveness, large scanning area and thus comparably high scanning speed (especially for cone beam based systems like the nanotom) are unfortunately still quite often not known or neglected.

The purpose of this work is to show the potential of high resolution laboratory CT scanners as a powerful complementary approach, to support the costly, time consuming and complex examination at synchrotron facilities. In the following the comparison of datasets obtained with both, an absorption contrast SRµCT setup and a state of the art high resolution cone beam laboratory scanner will show the unique properties of both approaches. The advantages (and limitations) of both methods are shown at several example specimen with high and low absorption characteristics. These cover the materials science sector as well as the biomedical world.

2. The CT systems

2.1 The phoenix nanotom laboratory CT system

The nanotom was introduced in 2006 by phoenix|x-ray in order to cover the growing demands for a compact laboratory CT system for spatial resolutions which could up to then only be reached by synchrotron radiation based setups on the one hand. On the other it should give the user extreme high flexibility for applications in fields such as materials science, micro mechanics, electronics, geology, and biology to name a few. Therefore, it is particularly suitable for examination of sensors, complex mechatronic samples, microelectronic components as well as for material samples such as synthetic materials, ceramics, sintered alloys, composite materials, mineral and organic samples.

In order to cover the widest possible range of samples the system is equipped with the first commercially available 180kV high power nanofocus (HPNF) tube. This source can be operated in four different modes. On the one hand in the so called nanofocus mode it provides an X-ray spot size of down to approximately < 0.9 µm which can be used for highest resolution CT scans with submicrometer voxelsize. Due to the penumbra effect the spot size predominates the images sharpness for extreme magnifications (for details see e.g. [11]). In Fig. 1 (a) the resolution capability of the high power nanofocus source is demonstrated. It shows that the 0.6 µm structure (line width) of the so called JIMA test pattern (designed by the **J**apan **I**nspection Instruments **M**anufacturers' **A**ssociation for testing high resolution X-ray equipment [12]) can clearly be resolved with more than approximately 20% of the CTF, showing the X-ray source size can be as small as below 0.9 µm.

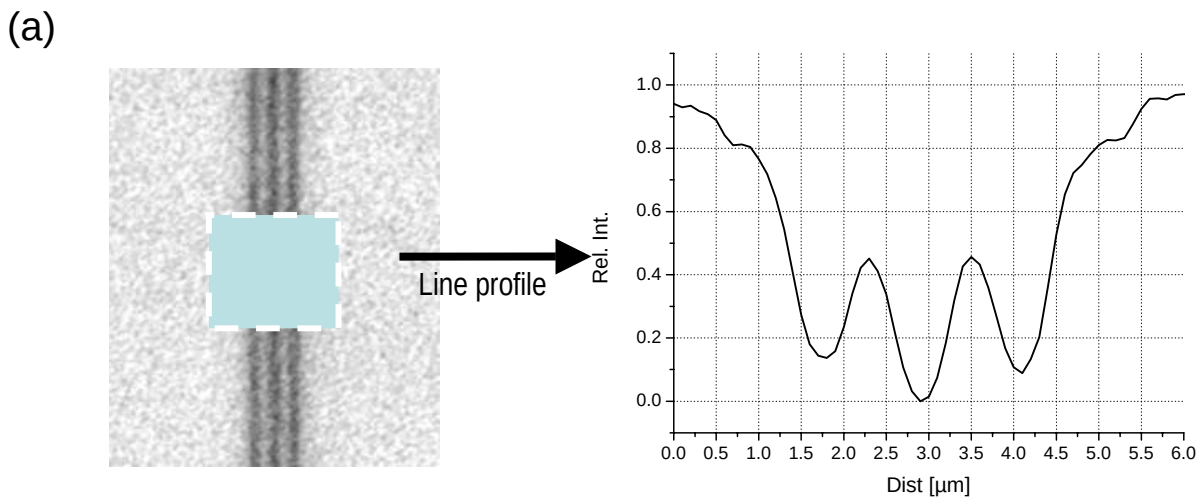

Fig. 1: X-ray images of test patterns showing the capabilities of resolution and detail detectability of phoenix|x-ray's high power nanofocus tube. In (a) the 0.6 µm line pair structure of the JIMA test pattern is clearly resolved

In the high power mode (up to 15 Watts at the target) on the other hand, the tube has enough penetration power to examine high-absorption samples like copper, steel or tin alloys and thus allowing e.g. the analysis of new connection systems for electronic devices or high absorbing geological samples, etc. The tube is equipped with a so-called transmission type target. This means the target is a thin layer (a few microns) of W or Mo which has been sputtered on the Be exit window which is hit by the focused electron beam. For the transmission geometry the X-rays are emitted in the same direction as the incoming electron beam.

On the detection side a 5-megapixel flat panel CMOS detector with a GOS scintillator deposited on a fiber optic plate is used. The pixel size of 50 µm and a 3-position virtual detector (i.e. 360 mm detector width) give rise to a wide variety of experimental possibilities. To avoid any potentially negative influence of vibrations or thermal expansion, tube, detector and manipulator are mounted on a granite structure. Furthermore, special materials and construction details for e.g. the tube mounting are used to minimize the variation of the focal-spot/detector distance during a scan. In addition, minimal vibrations of the system are suppressed by the air bearing of the rotation unit. A tube cooling is available to suppress thermal influences during the CT scan.

For reconstruction of the volume data GE Sensing & Inspection Technologies uses a proprietary implementation based on Feldkamps cone beam reconstruction algorithm [13]. The reconstruction software contains several different modules for artifact reduction (e.g. beam hardening, ring artifacts, drift compensation) to optimize the results. In Fig. 2 the effect of the ring artifact suppression method is shown. In the figures two identical cross sections of a cortical bone sample (human bone) scanned with the nanotom at 90 kV and 150 µA and 1.8 µm voxelsize are shown. The original study was performed by M. Dalstra et al using the SRµCT setups at HASYLAB/DESY. The study was performed to quantitatively evaluate the remodeling process in osteoporotic cortical bone [14]. For quantitative analysis of the datasets it is essential to minimize the artifacts in the reconstructed volume. As can bee seen in Fig. 2 the approach implemented by phoenix|x-ray effectively eliminates the ring artifacts and therefore a further quantitative analysis could also be performed on the nanotom CT datasets as it was done with the results of the SRµCT scans. One remarkable result of the shown nanotom data is the high contrast resolution which even allows a separation of the different density phases in the bone.

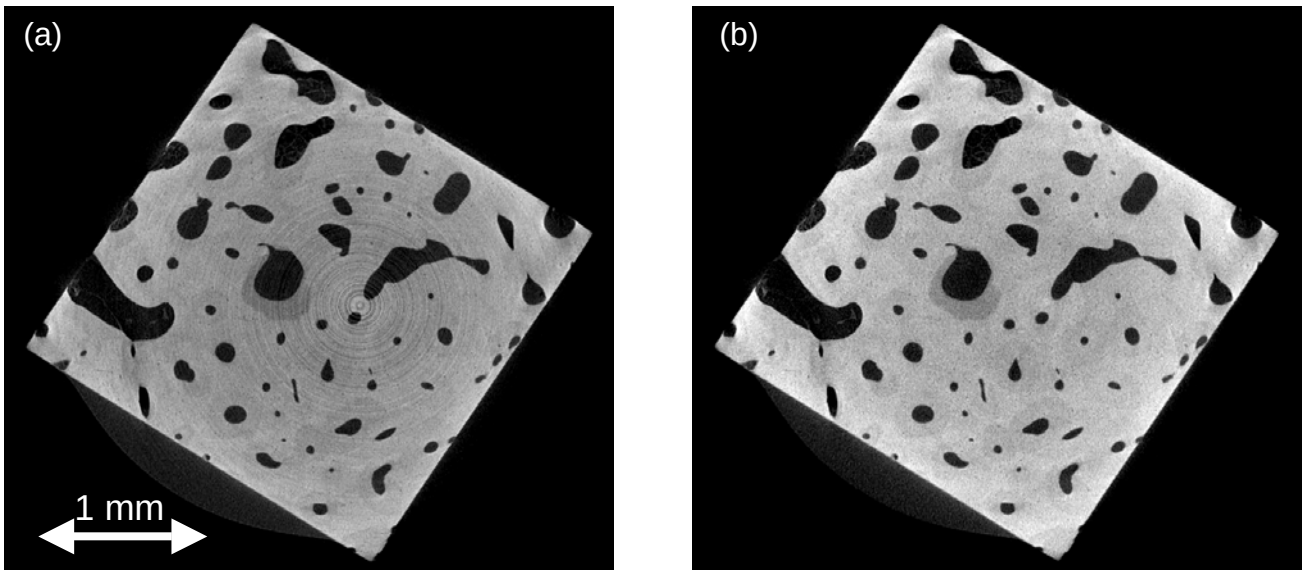

Fig. 2: Cross section of cortical bone sample scanned with the nanotom. Due to an effective ring artifacts suppression a segmentation of the different phases in the bone structure becomes possible.

2.2 The Synchrotron CT setup

The SRμCT measurements were carried out at the 2nd generation storage ring DORIS III at HASYLAB/DESY in Hamburg/Germany. Two different beamlines have been used. For specimen with lower absorption coefficients like e.g. biomaterials polymers or ceramics the CT setup was installed at the beamline BW2 using photon energies in the range of 8 to 24 keV. For the investigation of larger samples and for samples consisting of stronger absorbing elements the apparatus was modified and installed at the high-energy beamline HARWI-II, operated by GKSS-Research Center Geesthacht/Germany, for the use of higher photon energies ranging from 20-250 keV. The technical description of the beamline is given in [15]. Especially for the investigation of high absorbing samples in the field of materials science, e.g. studying the plastic flow in friction stir welds, and medical application, e.g. implant material in bone, the use of higher photon energies becomes mandatory. The setup used for absorption-contrast microtomography is presented in detail in [16] and [16]. It consists of a 2-dim. X-ray detector and a sample manipulator stage. The sample manipulator provides both for the rotation and for the lateral positioning of the specimen. The incident X-rays are converted into visible light (scintillator: $CdWO_4$ single crystal, thickness 200μm - 1000μm) which then is projected onto a CCD camera (KX2, Apogee Instruments, Inc.; 14 bit digitalization at 1.25 MHz, 1536 x 1024 pixel) by an optical lens system. The spatial resolution limit for CT examination at both beamlines is approximately 2 μm. After performing the CT measurements a new tomography instrumentation dedicated for beamline HARWI-II was installed. By including new CCD cameras with 16 bit digitalization together with a new sample manipulator stage based on air bearing the density resolution and the throughput of the system could be increased.

For absorption-contrast microtomography typically a set of 720 radiograms at different sample rotations equally stepped between 0 and 180° were taken. The tomographical reconstructions are calculated by using the backprojection of filtered projection algorithm.

3. Samples and Scanning Parameters

Twodifferent sample types have been chosen to be studied by SRμCT as well as high resolution conventional CT. Identical regions of the specimen described in the following have been scanned by both systems. In order to allow a quantitative comparison, the resulting volume data had to be

registered to each other using either a software described also in this proceedings in [18] or VGStudio MAX 2.0 by Volume Graphics in Heidelberg/Germany.

3.1 Sample 1: Cu/Al_2O_3 catalyst

Impregnation of pre-shaped metal oxide particles is one of the most applied preparation procedures of industrial heterogeneous catalysts. Different mathematical descriptions of the impregnation step have been developed. However, radial profiles have been seldom measured in practice. One recent report shows the SRμCT datasets used for the present study [19]. Cu/Al_2O_3 catalysts, differently impregnated with $CuCl_2$-solution as described in ref. [19] and using alumina pellets of the same shape and size, were investigated. For the present study a cylindrical porous Al_2O_3 catalyst (3.3 mm diameter, 4 mm height) was immersed for 1 min in the impregnation solution. This sample was used to evaluate the contrast resolution of the nanotom. One goal was to find out if as show in [19] for the SRμCT scans the position of the $CuCl_2$ diffusion front can be identified also with the laboratory CT system. Furthermore the fine grains of the specimen allow a qualification of the spatial resolution capabilities of the nanotom.

3.2 Sample 2: Sintered Ti6Al7Nb

This alloy is especially interesting as potential material for bone implants. In a GKSS research project the potential of this material class for medical application is evaluated. Goal of the CT scans is to analyze the 3D morphology of sintered porous Ti6Al7Nb. For the CT examinations four cylindrical specimen (3.5 mm diameter, 5 mm in height) have been produced from spherical Ti6Al7Nb particles. The particle diameter was as follows: sample (a): 45-75μm, sample (b): 75-90μm, sample (c): 90-125 μm and sample (d): 180-250 μm. The high absorbing Ti6Al7Nb samples have been scanned to show the capabilities of the laboratory system at higher acceleration voltages. It should be shown that within a rather short scanning time high resolution CT datasets of high absorbing materials can be obtained with the nanotom.

3.3 Overview of the CT parameters

An overview of the parameters which have been used for the nanotom and the SRμCT system are shown in the tables one and two, respectively.

Table 1: Parameters of the nanotom scans

Sample	**Sample 1: Cu/Al_20_3**	**Sample 2: Ti6Al7Nb (sample d)**
Acceleration Voltage	60 kV	100 kV
e-beam current	240 μA	60 μA
Tube operation mode	1	0 (High Power)
X-ray filter	0.1 mm Cu	0.5 mm Cu
Focal spot size	< 2 μm	< 3 μm
Voxel size	2.5 μm	4.5 μm
scanning volume	5x5x4.5 mm^3	5x5x4.5 mm^3
Angular increment	0.12°	0.36°
Scanning time	160 min	20 min

As it can be seen in table 1, the tube of the nanotom was not operated in the nanofocus mode (mode 3) for the presented test samples. The size of the test samples physically limits the achievable magnification and thus voxelsize for scanning the complete sample for both systems (laboratory CT

and SRμCT scans) and thus it was not necessary to use the nanofocus mode. Results with subμm voxelsize and nanofocus mode are e.g. shown in [11] or [10].

Table 2: Parameters of the SRμCT scans

Sample	**Sample 1: Cu/Al_20_3**	**Sample 2: Ti6Al7Nb (sample d)**
Beamline	BW2	HARWI-2
Photon Energy	18 keV	65 keV
Spatial Resolution (10% MTF)	4 μm	13.5 μm
Voxel size	2.3 μm	2.7 μm
scanning volume	3.5x3.5x2.3 mm^3	4.1x4.1x2.7 mm^3
Angular increment	0.25°	0.25°
Scanning time	160 min	90 min

The tables indicate one obvious advantage of the laboratory scanner. The achievable throughput (i.e. sample volume per time) is between 4 and 10 times higher for the nanotom. This is mainly attributed to fact that the cone beam geometry of the laboratory CT system covers a much larger scanning area than the parallel beam geometry of the SRμCT setup. The much lower flux of the X-ray tube is partly compensated by the comparably large detector pixel size (50 μm) and the high quantum efficiency of the flat panel detector. For the SRμCT setup it has to be noted that at the performed scans most of the scan time is used for alignment and calibration to obtain a high spatial and density resolution in the tomogram. The comparison of the actual results is given in the next section.

4. Results and Discussion

In order to allow a direct and quantitative comparison of the datasets obtained by the two different setups first of all the datasets had to be aligned to each other. Sample orientation and position can obviously be very different for two scans of the same specimen. In order to allow a best fit registration the first step for the registration is a manual alignment using either (a) the software tool developed by Beckmann et al. described in [18] or (b) VGStudio MAX 2.0. Sample 3 was registered using method (a). For the samples 1+2 method (b) was chosen. For this method one first of all loads both datasets into VGStudio. Now prominent features (like larger high absorbing particles) are identified in both datasets to allow an easy manual pre-registration by shifting and rotating. Finally, a best fit algorithm is used to get the optimal registration of the datasets.

4.1 Cu/Al_20_3 catalyst

Sections of the CT datasets of the Cu/Al_20_3 catalysts are show in Fig. 3 for the nanotom scan on the left (a), for the SRμCT scan on the right, respectively. Looking at values for voxelsize and 2D resolution of both scans in the tables 1 and 2 (for the case of the nanotom with a spot size which is below the voxelsize a 2D resolution close to the value given for SRμCT scan can be estimated) a comparable spatial resolution for the CT datasets can be expected. Both the 3D rendered image and especially the part of the cross section below clearly show that the difference in spatial resolution of the scans is below 0.5 μm. Gaps between the grains down to 3-4 μm can be identified in both scans.

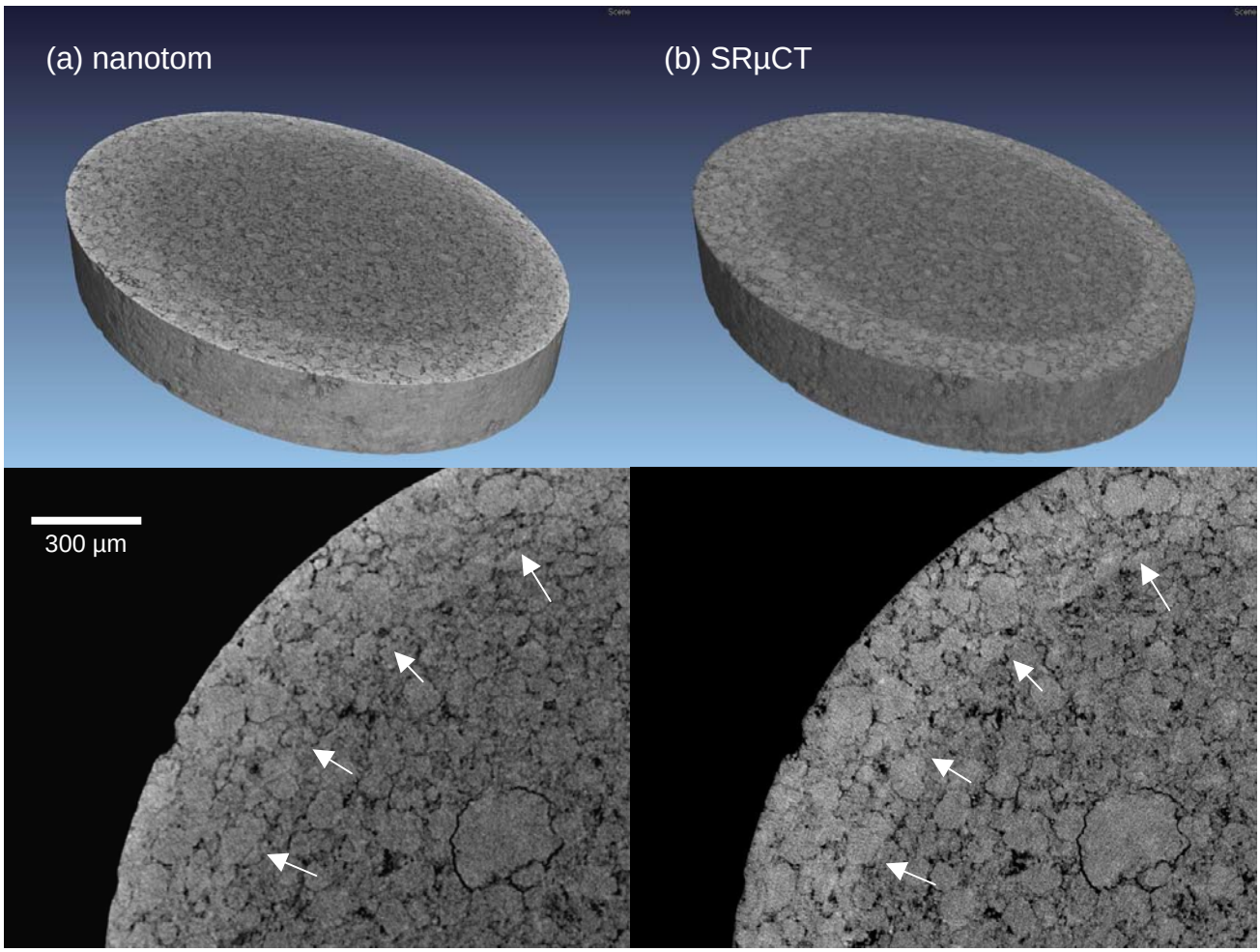

Fig. 3: Comparison of the CT results of the Cu/Al_2O_3 specimen. In both scans the outer ring like zone (white arrows) which has been infiltered by the $CuCl_2$ can be observed. Whereas the spatial resolution appears very similar, the border of this zone is more obvious in the SRµCT scan due to the superior contrast resolution.

The images indicate also a comparable data quality with respect to ring artifacts (almost no such artifacts can be found) and signal to noise ratio.

One major goal of the CT examination of the Cu/Al_2O_3 specimen was to measure how deep the $CuCl_2$ has diffused into the porous ceramic matrix after different immersion times. As it can be seen in Fig. 3(b), the higher absorbing Cu can easily be found in the SRµCT datasets (the ring like structure at outer part of the cylinder) and a sharp end of the diffusion front can be identified. In case of the nanotom dataset (a) it is obvious that also with the polychromatic X-ray source of the nanotom it is possible to separate the Cu filled outer part of the specimen from the inner Cu free section. However, a small decrease in absorption coefficient from the border to the center of the sample can be found which can be attributed to beam hardening. This artifact is also referred to as cupping effect. A stronger pre-filtering of the source spectrum and/or additional software filters as described in the next section could further reduce this effect.

4.2 Sintered Ti6Al7Nb particles

Out of the three examples this specimen showed by far the highest absorption behavior. Therefore in order to achieve proper penetration of the sample and an optimal scan result it was necessary to use relatively high acceleration voltages (100kV) for the X-ray tube and also a high photon energy (65 keV) for the SRµCT measurement. In order to protect the lens system of the current absorption contrast SRµCT setup at higher photon energies a thicker (1mm) $CdWO_4$ crystal has to be used. On

the one hand this has the advantage to increase the quantum efficiency of the setup, on the other the thicker screen limits the resolution for such scans as information is smeared out on the scintillator. Therefore even if the voxelsize for the SRµCT dataset is a factor of about 1.7 smaller than for the nanotom data, the achieved spatial resolution is better for the laboratory scanner as it is shown in figure Fig. 4.

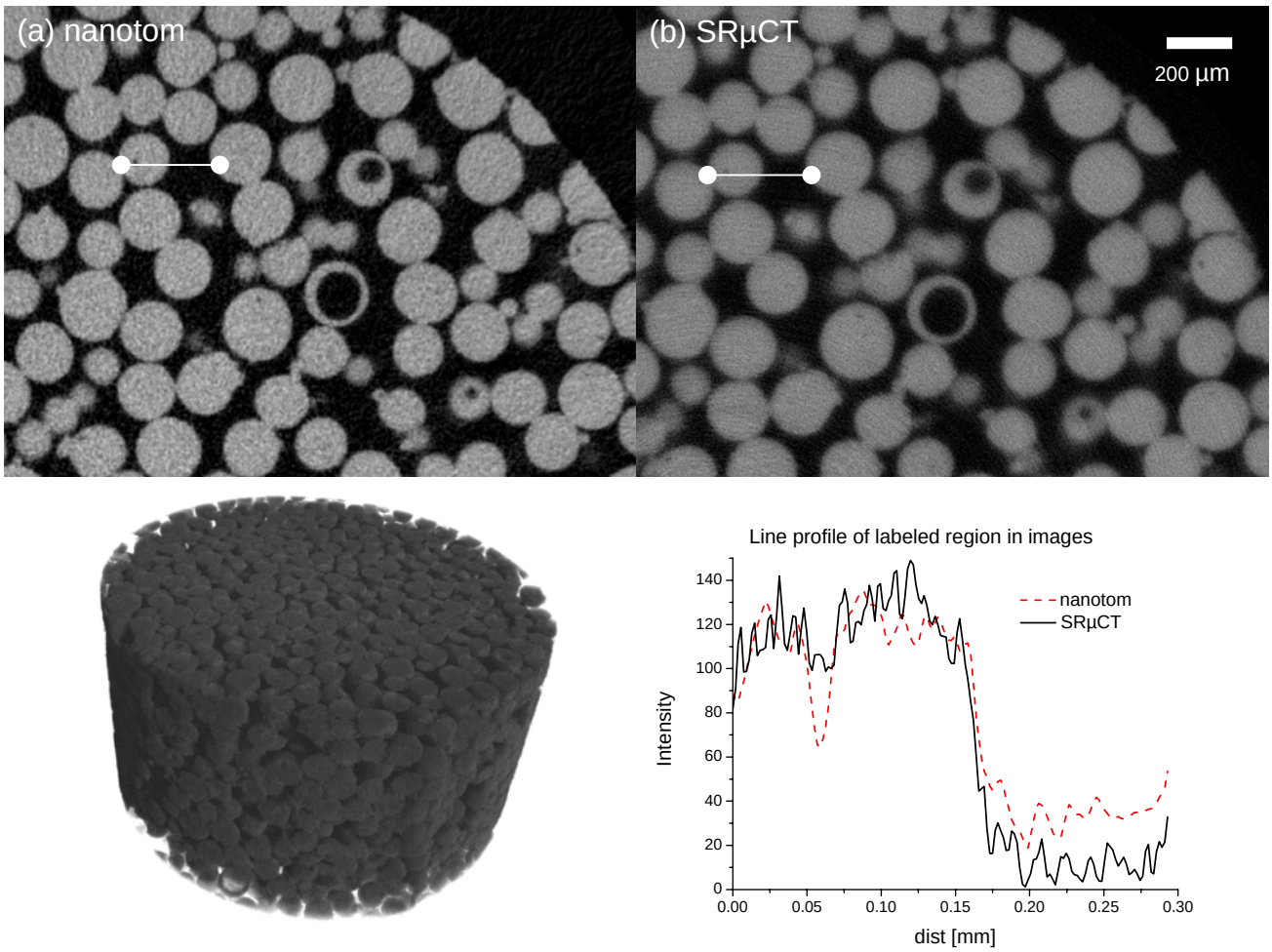

Fig. 4: CT results of the Ti6Al7Nb scans. The line profile confirms the higher resolution of the nanotom scan.

A direct comparison of a line profile clearly shows the higher spatial resolution of the tube based scan data. In a different setup at HASYLAB uses mirror system to protect the optical lenses from the higher harmonics of the direct beam. This allows to implement thinner scintillator crystals. Therefore an improved spatial resolution also for higher energies can be expected.

5. Summary and Outlook

The present study aimed to show a comprehensive comparison of CT scans obtained with a commercial high end CT scanner with a nanofocus X-ray tube and a absorption contrast synchrotron radiation based CT setup. Two samples with different absorption characteristics (a porous Al_2O_3 catalyst and a sintered Ti6Al7Nbsample) have been scanned in a voxel size range between 2.3 and 10 µm. The chosen specimens are good examples for typical application of both systems. In order to allow a direct and easy comparison of the results, the scan data has been registered to each other by a best fit algorithm. The analysis of the scans reveals that the nanotom gives excellent data quality which in many cases can even compete with SRµCT data. For the shown examples the spatial resolution and also the signal to noise ration of the two systems was absolutely comparable. As the resolution limit of the used SRµCT setup at HASYLAB/DESY was

limited to 2µm, it was not possible to compare nanotom data with subµm voxelsize to corresponding SRµCT data right now. The next step will be a comparison of nanotom data at the resolution limit of the system which is below 0.9 µm with the data from the next generation SRµCT setup at the new third generation source PETRA III at DESY which is now available.

In total the major pros of the laboratory scanner are its large field of view, large scanning volume, high penetration power due to the 180kV tube, scanning speed (scanned volume per time), ease of use and overall cost effectiveness. The synchrotron radiation CT on the other hand provides an excellent contrast resolution, precisely adjustable monochromatic radiation and therefore no beam hardening artifacts. In conclusion, state of the art conventional high resolution CT scanners like the nanotom by phoenix x-ray can adequately support and complement research projects where high quality CT data is required. Due to its flexibility the nanotom can be used for both, extreme high resolution scans with subµm voxelsize of small samples on the one side or also fast scans of high absorbing (or larger) specimen using the high power mode on the other. Thus an ideal situation for such projects is to use both systems. For subµm scans or studies where a lot of samples have to be scanned the nanotom will be used. Whereas for situations in which optimal contrast resolution or artifact free data is needed, the synchrotron radiation based CT would be the system of choice.

Acknowledgments

We thank DESY for providing the photons at the storage ring DORIS-III and the operation of beamline BW2. Thank also goes to J.-D. Grunwaldt, Technical University of Denmark, Lyngby, Denmark, for providing the Al_2O_3 sample. For the sintered TiAlNb particles we thank F. Feyerabend and R. Willumeit, GKSS. For the bone sample presented in Figure 2 we thank M. Dalstra and P.M. Cattaneo, University of Aarhus, Denmark.

REFERENCES

[1] Roth, H. Mazuik B., “What you can’t see can hurt you”, Quality Test and Inspection, 5, (2003)
[2] Moller – Gunderson, D., “When 2D X-ray isn’t enough” SMT , 8, (2007).
[3] Nier, E., Roth, H., “Analysis of Crimp Interconnections by Microfocus Computed Tomography” XXX, 2004.
[4] Bonse, U., (Editor.), “Developments in X-Ray Tomography IV” SPIE, Wellingham WA, (2004).
[5] Bonse U., (Editor.), “Developments in X-Ray Tomography V”, SPIE, Wellingham WA, (2006).
[6] Obrist, A. et al., “First Article Inspection Based on Industrial X-ray Computed Tomography”, Materials Testing and Research, International Conference, Nuremburg, 177-180 (2001).
[7] Brunke O., “Dimensionelles Messen mit hochauflösender 3D-CT“, QZ, 62-64 (2008).
[8] Suppes, A., Neuser, K., „Metrology with µCT: precision challenge” in Developments in X-ray Tomography VI, edited by Stuart Stock, Proceedings of SPIE Vol. 7078, (2008)
[9] Bonse U., Busch F., „X-ray computed microtomography (µCT) using synchrotron radiation (SR)., Prog. Biophys. Mol. Biol., 65(1-2), 133-169 (1996)
[10] Withers, P., “X-ray nanotomography”, Materials Today, 10(12), 26-34 (2007)
[11] Brockdorf, K. et al., “Sub-micron CT: visualization of internal structures” in Developments in X-ray Tomography VI, edited by Stuart Stock, Proceedings of SPIE Vol. 7078, (2008).
[12] Japan Inspection Instruments Manufacturers' Association, http://www.jima.jp
[13] Feldkamp, L.A., Davis, L.C., Kress, J.W. “Practical cone-beam algorithm”, Journal of the Optical Society of America A, 1(6), 612-619 (1984)
[14] Dalstra, M. et al., “Osteonal mineralization patterns in cortical bones studied by synchrotron radiation-based computed microtomography and scanning acoustic microscopy”, in Developments in X-ray Tomography IV, edited by U. Bonse, SPIE Vol. 5535, 143-151 (2004)
[15] Beckmann, F., et al., “New developments for synchrotron-radiation-based microtomography at DESY”, in Developments in X-ray Tomography V, edited by U. Bonse, SPIE Vol. 6318, 1-11 (2006)
[16] Donath, T., “Quantitative X-ray Microtomography with Synchrotron Radiation”, GKSS-Forschungszentrum Bibliothek, Geesthacht, (2007)

[17] Davis, A., R., Bush, C., Harvey, J. C. and Foley, M. F. , "Fresnel lenses in rear projection displays," SID Int. Symp. Digest Tech. Papers 32(1), 934-937 (2001).
[18] Drews S, et al, “Three dimensional characterization of the bone-cartilage interface using micro computed tomography” in Developments in X-ray Tomography VI, edited by Stuart Stock, Proceedings of SPIE Vol. 7078, (2008).
[19] Grunwaldt, J.-D., Beckmann, F. and Baiker, A., “Application of X-ray microtomography in catalysis: A study of shell-impregnated solid catalysts”, HASYLAB annual report, www-hasylab.desy.de, (2007).
[20] Kak, A.C., Slaney, M., “Principles of computerized tomographic imaging”, New York, IEEE Press, (1988)
[21] Brunke, O., Odenbach, S., Beckmann, F., “Quantitative structure analysis of aluminium foams by means of µCT”, Eur. Phys. J. Appl. Phys. 29(73) (2005)
[22] Sakellariou, A., et al., “Developing a virtual materials laboratory", Materials Today 10(12) 44-51 (2007)